Jordan S, Baker NJ, Washington JG, Atkinson GJ, Pinguey E.

Construction methods for modulated pole machines.

In: Electric Machines and Drives Conference (IEMDC). 2017, Miami, FL, USA: IEEE.

DOI link to article:

https://doi.org/10.1109/IEMDC.2017.8002068

Date deposited:

29/08/2017

Construction Methods for Modulated Pole Machines

Steven Jordan[1], Nick J. Baker[1], Jamie G. Washington[2], Glynn J. Atkinson[1] and Edwin Pinguey[1]
[1]Electrical Power Group, Newcastle University, Newcastle, United Kingdom
[2]Electromagnetic Applications, Höganäs AB, Höganäs, Sweden

***Abstract*—The modulated pole machine (MPM) is known to offer high torque density utilizing permanent magnets and a three dimensional flux pattern. However, their construction requires a departure from conventional coil wound teeth formed of lamination stacks which can be a challenge. In this paper three construction techniques for MPM stators are compared: pure soft magnetic composite, pure lamination and a hybrid of the two. Simulation and practical knowledge of the build of each of these machines, including torque capability and mechanical tolerances is presented and discussed. Using the methods proposed here, it is shown that the pure laminate MPM machine has the potential to offer the greatest torque per kg of active material, yet it is the hybrid machine which delivers the highest absolute torque.**

Keywords—Modulated Pole; Transverse Flux; Construction Methods

I. Introduction

The concept of modulated pole machines (MPM) comprises highly permeable iron structures around a single homopolar coil, creating a multiplex of poles each with an MMF equal to that of the homopolar coil. Increasing the pole number results in an increase in the magnetic field strength produced by the poles and this in turn results in an increase in the specific torque. This acronym is introduced to gather together a range of machines known by a variety of titles which use this principle. A particular example is the transverse flux machine (TFM), which has its origins in two papers presented by Weh [1, 2]. These papers make reference to the fact that flux links with the windings in a direction which is 'transverse' to the direction of the machine's motion, whereas conventional layouts have major elements of their flux paths more in alignment with the motion direction of the machine. It is argued that TFM is an inadequate name as it fails to recognize the crux of this family of machines, which is in the method of making multiple poles from single coils.

MPMs are gaining favor in low speed, high torque applications [3-6]; however, their construction can vary quite dramatically. There is no typified structure, with some favoring C-core stator assemblies constructed solely from a laminate material [7], other topologies consider some - or all - magnetic parts made from soft magnetic composite (SMC) materials [8, 9] providing extra degrees of flexibility in component design, whilst further examples contain claw-pole or claw-pole type structures [10, 11]. It is unclear which construction method provides the best possible solution for a range of applications as the requirements can constrict the possibilities available. Commonality occurs in the toroidal winding but this poses problems where leakage paths yield a low power factor [12]. Cogging torque is another issue, occurring due to the high pole numbers involved and their desire to align with the path of minimum reluctance. Techniques exist to reduce this effect, such as those detailed in [13], but they are not discussed for the single phase machines explored in this paper.

This work was conducted under the Engineering Doctorate programme supported by Höganäs AB

II. Materials for Modulated Pole Machines

Several approaches can be taken with regards to the construction of modulated pole machines, therefore the material selection for each differs. This section discusses the approach taken in material selection for MPMs.

A. Solid Iron

Solid iron is mechanically the best option for manufacturing MPM structures. Different amounts of processing and alloy content of solid iron can produce a range of grades with different B-H characteristics. It can be satisfactorily used in machine components where there is little or no alternation in the flux – for example the claws of an automotive alternator. However, its use within MPM armature structures is limited due to the presence of alternating flux, which results in loss and, hence, heat being generated within the iron, the majority of which is as a result of eddy currents. Hysteresis loss is generally reduced by controlled processes in the manufacture of the iron itself, such as the reduction in contamination.

B. Laminated Iron

The conventional method of limiting eddy currents is to laminate the iron structures, with a thin layer of electrical insulation between each lamination. This limits the size of the path an eddy current can take and reduces the resistive loss it contributes. While the dielectric used to insulate adjacent laminations is normally applied as a thin coating and is a small fraction of the thickness of the lamination, the process of stacking laminations creates air-gaps: Issues exist with an accumulation of parasitic air-gaps, which can alter permeable paths, cause thermal hotspots and localized degradation. This lends laminations well to topologies which are a linear extrapolation of a 2D geometry, such as most conventional cylindrical machines. However, in cylindrical MPM machines, the geometry for the lamination is normally extrapolated in the circumferential direction, which is difficult to realize in manufacturing. Laminations can be made in the axial plane but require a core-back laminated in the orthogonal plane aligned with the path of flux [7].

C. Soft Magnetic Composite

Often MPMs take advantage of the isotropic properties of SMC to produce machines that still have modular construction, but the individual parts are in contact with each other, utilizing space better in the machine. The isotropic properties of SMC are achieved by performing the same process as laminating, but in all three dimensions and at a micron scale. Powdered iron with grain sizes of the order of 50 µm is mixed with a dielectric, insulating the individual grains from each other. The powder is then compressed at high pressures to form a solid and is heat treated to stress relieve the part: at low enough temperatures to avoid sintering, which would destroy the insulation. Hence, this reduces hysteresis loss and also develops the insulation, which in part is an oxide. The result is a part that requires no post-processing and is laminated in all directions at a microscopic level, limiting eddy current flow to within individual grains.

There are drawbacks to the SMC material: a low mass density - circa 7400 kg/m^3 depending upon material grade - results from limits on the compaction pressure during manufacture. If the pressure is too high, it starts to significantly breakdown the insulation between adjacent particles, allowing larger eddy currents paths to be formed. Prototyping in SMC is difficult and the aspect ratio of components must be adequately considered for the limit of what can be compacted. The aspect ratio is important to guarantee a uniform density can be achieved throughout the material. It is recommended that the available surface area exposed to the press is larger than the pressing length by a factor of 6:1 or greater. This will overcome the issue of friction with the die walls preventing proper compaction in the centre of the section. This results in lower densities, and an increased likelihood of cracking, in these regions.

Most SMC grades are specifically designed for pressing directly into component shapes and would lose some of their electrical performance characteristics if machined after heat treatment. It is possible to machine the components prior to heat treatment, known as the green state, but this has the potential to distort the component shape upon post machining heat treatment. A prototyping SMC material has been developed specifically for machining. It is pre-heated giving it good mechanical properties when compared to green state. However, this mechanical flexibility comes at the expense of inferior electromagnetic properties, as shown in *Table I*.

TABLE I. HÖGANÄS SOMALOY® MATERIAL PROPERTIES

Material ID	Resistivity (µΩ·m)	Mass Density (kg/m^3)	μ_{MAX}	B @ 10 kA/m (T)
Prototype	280	7300	430	1.46
130i 1P	8000	7350	290	1.40
700HR 1P	1000	7450	440	1.53
700HR 5P	700	7500	600	1.57
1000 3P	70	7560	850	1.63

III. CONSTRUCTION METHODS

This section describes the different construction methods for three, single-phase prototypes, which follow the specification set out in *Table II*.

TABLE II. DIMENSIONS OF PROTOTYPE

Dimension	Quantity	Unit
Number of Poles	50	-
Axial Length	24	mm
Stator OD	188	mm
Air-gap Length	0.5	mm
Air-gap Diameter	155	mm
Winding Axial Thickness	8	mm
Magnet Grade	NdFeB N38H	-
Magnets (l x h x w)	24 x 6 x 3	mm

A. Stator Type 1: Hybrid SMC Laminate

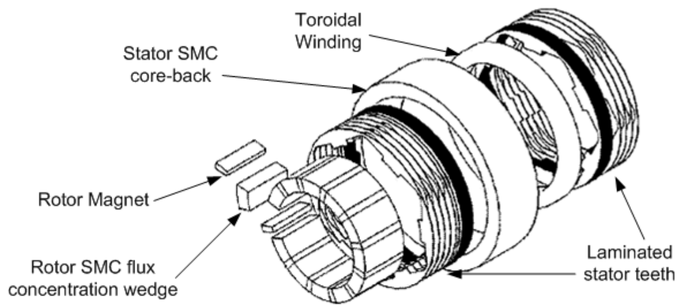

Fig. 1. Hybrid SMC Laminate Machine Exploded View

The stator consists of two lamination stacks which modulate the coil driven flux and have been produced using a rolled up strip concept: the laminated stator teeth, depicted in Fig. 1, are cut as a long chain which is then formed into a circular ring thus reducing waste material from an internal bore stamping method. These two stator stacks sandwich a toroidal winding. The core-back has three dimensional alternating fields and hence it was manufactured from SMC segments. A punch and die for the part is not justifiable for the prototype on cost grounds and, hence, the core-back was machined from rectangular billets of Somaloy® prototype material. For the prototype machine, the core-back was manufactured as a series of ten arcs: each arc section being machined in its pre-heat treated green state. Heat treatment was performed post machining to remove built-up stress in the part during the pressing process. The arcs deformed slightly in the heat treatment process, straightening marginally: this resulted in a larger radius and a loss of concentricity. The teeth section is laminated and it carries the field radially - and to some extent circumferentially - from the air-gap and onwards into the core-back. This ring allows the flux to spread evenly across the laminations and take the shortest route across the core-back, which is not parallel to the axial direction. A pole pitch displacement circumferentially between the two lamination stacks means the rotor does not have to be skewed, shown in Fig. 2. The use of laminations in the axial direction aims to reduce armature leakage flux flowing axially across the machine and, hence, improve the power factor.

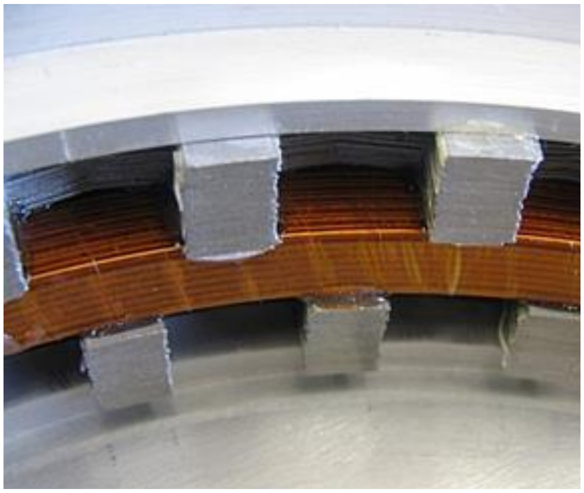

Fig. 2. Hybrid SMC Laminate Machine Prototype

B. Stator Type 2: Formed Laminations

The aim of the formed lamination concept is to simplify the stator construction by reducing the part count and parasitic air-gaps through the elimination of the SMC core-back. Toothed lamination stacks are instead combined with a single core-back linking the opposing poles and formed from a single laminated component.

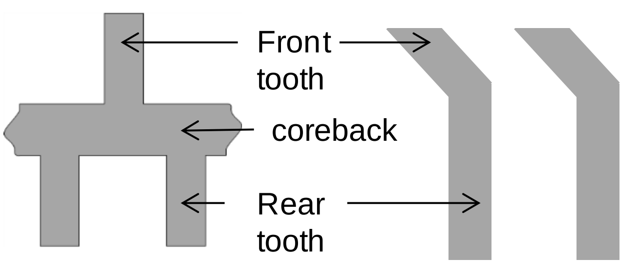

Fig. 3. Formed Lamination Machine 2D View (with and without Core-back)

There is no electromagnetic requirement for a single continuous core-back spanning the entire machine circumference, as shown in the left hand side of Fig. 3. The right hand side of Fig. 3 produces the same modulating effect with no core-back. Fig. 4 shows how in practice, for mechanical reasons, adjacent teeth need to be connected by a circumferential element, which can be located on the sides of the folded structure rather than the core-back.

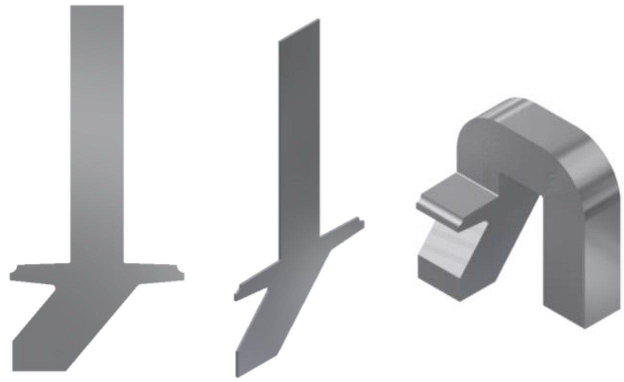

Fig. 4. Formed Lamiation Final Design

Implementation of this concept relies on an appreciation of bending materials. When a bend is formed, the material is taken beyond its plastic limit resulting in deformation: the inner radius under compression and the outer radius under tension, with a neutral axis centred between the two. The deformation due to a right angled bend showed significant deformation at the internal radius in a trial bend using aluminium bar. Observing Fig. 5, each individual lamination is deforming in the same way as the solid bar, but due to the ratio of the width of the material in the plane of the bend to the thickness of a lamination across the bend, the deformation is not clearly visible to the naked eye. The result for the same tooth bending process with a stack of laminations can be seen in Fig. 6 where the refined process can encompass the coil successfully.

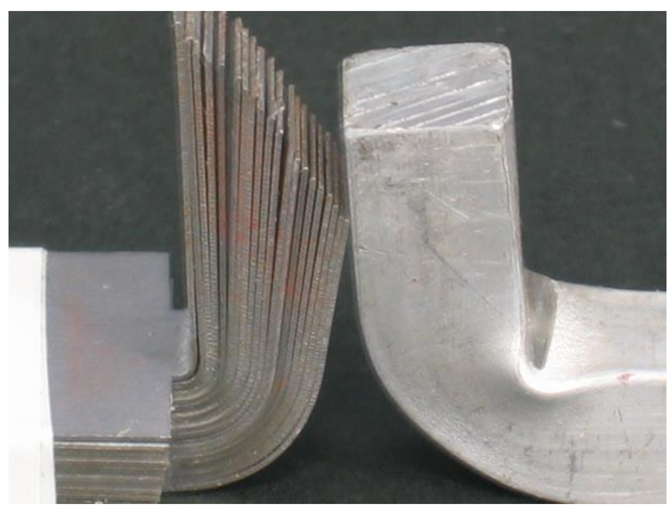

Fig. 5. Formed Lamination and Solid Material Bending Issues

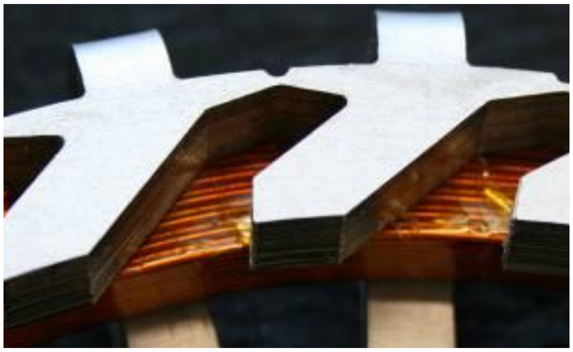

Fig. 6. Formed Lamination Machine Constructed

C. Stator Type 3: Full SMC

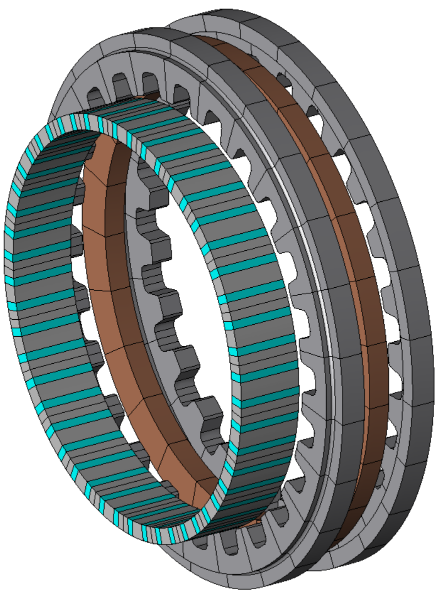

Fig. 7. Full SMC Machine

When fabricated from pressed SMC components, assembly of the stator involves the concentric mounting of pre-made hoop coil windings and the pressed toothed rings, as shown in Fig. 7. This yields a more simplistic assembly, where the SMC rings can be formed from the same pressing tool and stacked axially, with a circumferential offset, to form a phase set. A three-phase bicycle motor using this approach is depicted in Fig. 8. Producing pressing tools to accurately fabricate the stator SMC rings is an expensive procedure and, therefore, only components that can be mass produced are exploited for sintered and formed SMC components. Geometry can have a significant effect in the outcome of the part produced, where a feature of the structure can be no smaller than 2 mm minimum. This prevents deterioration of the materials under compaction pressures, where stress fractures can occur resulting in an incomplete component. Axial compression of the stator ensures no gaps between SMC rings.

Fig. 8. Full SMC Prototype Machine (External Rotor)

D. Coil

The coil is common across all the topologies and is a simple hoop shape sandwiched between the two stator sides giving a rectangular slot profile. It is a design objective to fill this slot with as much copper as possible and limit the air-gaps between the coil and the surrounding stator iron - both lamination and SMC - to improve the heat transfer from the coil.

The coil was wound from round enamel coated copper conductor. The sectional stator assembly and the simple rectangular cross section of the coil, coupled with the relatively low turn count (roughly twice the number of poles), facilitates well a preformed bobbin wound coil with ordered and structured turns and layers. Good copper fill and a reduction in asymmetry was achieved by the use of hard plastic punches to force the wire to the required position within a stiff former jig, maintaining good edge tolerance. A cut through of one of the prototype coils is shown in Fig. 9.

Fig. 9. Cross-section of Coil for Prototype

E. Rotor

The rotor structure is also common across the machine designs and uses magnets in a flux concentrated configuration: the magnets are alternately magnetized in the circumferential direction, separated by an SMC flux concentrating pole piece that orientates the flux for delivery to the stator tooth across the air-gap. In this application, the air-gap was fixed at 0.5 mm, detailed in *Table II*, as dictated by the maximum obtainable tolerance in-house. A stock of NdFeB N38H grade magnets was available and a working air-gap diameter of 155 mm was adhered to.

IV. Simulated Performance Comparison

The three prototypes for a single phase machine, depicted in this paper, are simulated and their performances compared based on static testing under no-load and the injection of DC current into the stator winding at different levels. Masses of each topology are also compared to indicate possible torque densities for scaled prototypes. The rotor mass remains constant since the magnets are predefined and thus the SMC pole pieces must also remain constant. Furthermore, the same copper winding is used for each machine topology, therefore, there is only the stator construction that will affect the masses of each machine.

In the hybrid machine, 0.2mm air gaps have been included between the stator teeth and core-back, in line with build experience (see Section V).

A. Mass

The results contained in *Table III* highlight that there is a considerable mass saving to be made from utilising the formed lamination approach. However, this is arguably the most difficult to manufacture and maintain tolerances throughout, particularly if scaling up. This is driven by the lack of coreback required in this configuration.

TABLE III. Mass Compairsons for the Three Machine Topologies

Machine Topology	Stator Mass (kg)	Rotor Mass (kg)	Winding Mass (kg)	Total Mass (kg)
Hybrid	1.17	0.51	0.44	2.12
Laminate	0.73	0.51	0.44	1.68
SMC	1.29	0.51	0.44	2.24

B. Back-emf

The back-emf of any machine is intrinsically linked to the torque. The laminate and SMC topologies perform almost identically, observed in Fig. 10, where the stator of the SMC machine is a high grade Somaloy material – 5P 700HR – which is comparable in performance with silicon iron. The hybrid machine suffers from mechanical tolerancing around the stator core-back/lamination interface, represented by a 0.2mm air-gap, which reduces the permeability of the structure and, therefore, the back-emf of this machine compared to the other two.

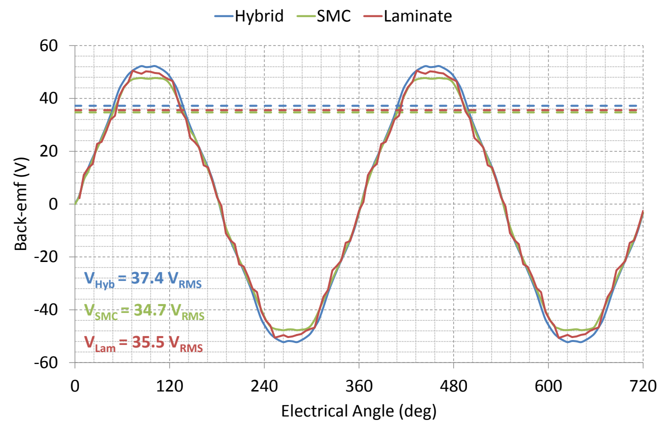

Fig. 10. Back-emf Profile for Machine Topologies

C. Cogging and Load Torque

Cogging torque is a common problem with modulated pole machines, where the high pole number and magnetic field strengths of flux concentrated magnets in this case, create significant reluctance forces. Around the detent points the laminate and SMC machines show behaviour that is expected with magnet fringing around the *q*-axis region, depicted in *Fig. 11*. However, the hybrid machine shows considerable variation as the iron stator poles align with rotor poles at a region of magnet flux leakage. This can be significantly reduced by controlling the tolerancing between the stator core-back and the lamination interface.

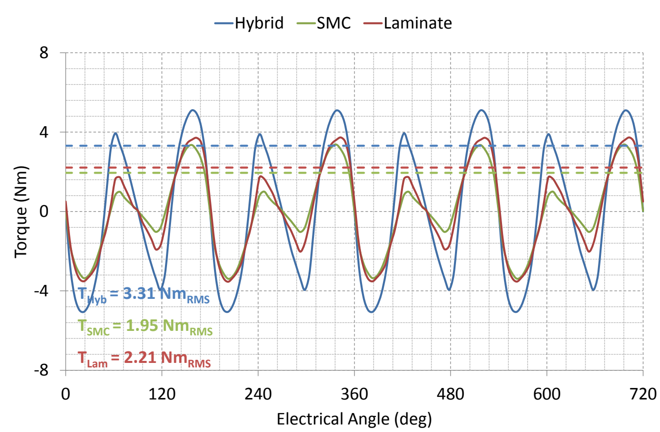

Fig. 11. Cogging Torque

Injecting current into the DC stator windings provides a static field to interact with the moving rotor field, providing an indication of the torque capability, as depicted in Fig. 12. The magnet forces, transitioning from the +*q*-axis and to the –*q*-axis, observed in Fig. 11, reduces the torque output in those regions of the hybrid machine but the RMS output is 6 % higher.

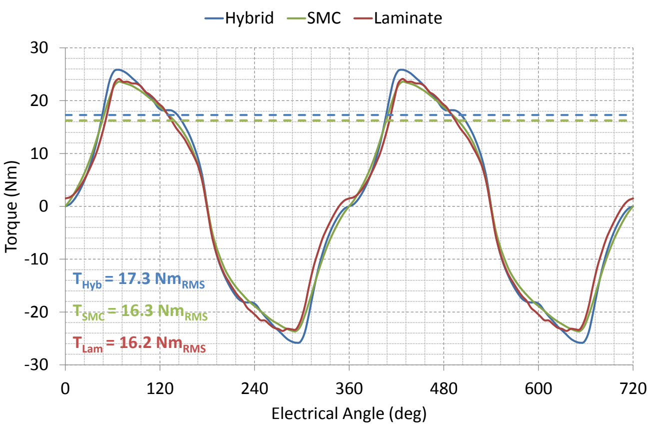

Fig. 12. DC Load Torque Profiles

D. Losses

The Joule losses can be quantified and are comparable across the three topologies, shown in *TABLE IV.* . Whilst the losses are low for both the hybrid and SMC machines, the complexity of the formed lamination machine leads to a problem in setting the lamination direction. Therefore, the eddy current paths can be calculated as larger than they actually are, leading to higher predicted Joule loss in the stator.

TABLE IV. JOULE LOSS DATA FOR THE THREE TOPOLOGIES

Machine Topology	Stator Loss (W)	Rotor Loss (W)	Winding Loss (W)
Hybrid	1.73	0.016	33.82
Laminate	2.95	0.027	33.82
SMC	1.73	0.029	33.82

The hysteresis losses were only accounted for in the iron loss condition applied to the laminate sections, yielding losses of 16.3 W and 12.2 W in the formed laminate and hybrid machine, respectively. It is expected that, at such low frequency, the hysteresis loss will be comparatively greater than the laminate sections, increasing the loss in the hybrid machine.

E. Power Factor

Neglecting saturation effects, then IX/E can be expressed as the flux ratio in (2):

$$\varphi_{pk}^{arm}/\varphi_{pk}^{mag} \quad (2)$$

where φ_{pk}^{arm} is the peak flux linkage due to the armature current and φ_{pk}^{mag} is the peak flux linkage due to the magnet.

Using the frozen permeability function, the flux linkages could be separated. For the armature driven flux, permeability of the stator was calculated and then re-run with the permeability frozen and the magnets defined as air. As stated in [14], there is no guarantee that the results in *TABLE V.* accurately account for the separation of the two contributing flux linkage sources without experimentally validating. The formed laminate model could not be accurately modelled in this instance owing to its complex geometry. Initial results imply the Hybrid version has a better power factor, driven by the parasitic airgaps adding to the reluctance of the φ_{pk}^{arm} path.

TABLE V. SIMULATED POWER FACTOR RESULTS

Machine Topology	Hybrid	Laminate	SMC
Power Factor	0.62	No Data	0.4

Increasing the pole number also increases the electric loading and this in turn can be expected to increase armature current driven flux and hence drive down the power factor, making the VA rating of the inverter rise. One of the major design goals of any modulated pole machine is, therefore, to find a geometry which limits armature driven flux without loss of magnet flux.

F. Force density

Combining torque and mass data from sections A and C, it is possible to calculate indicative torque densities. Defining the SMC machine as delivering 1 per unit torque per total active mass, the hybrid and pure laminate machines can be shown to deliver 12% and 33% extra torque per kg respectively.

V. HYBRID EXPERIMENTAL AND SIMULATION RESULTS

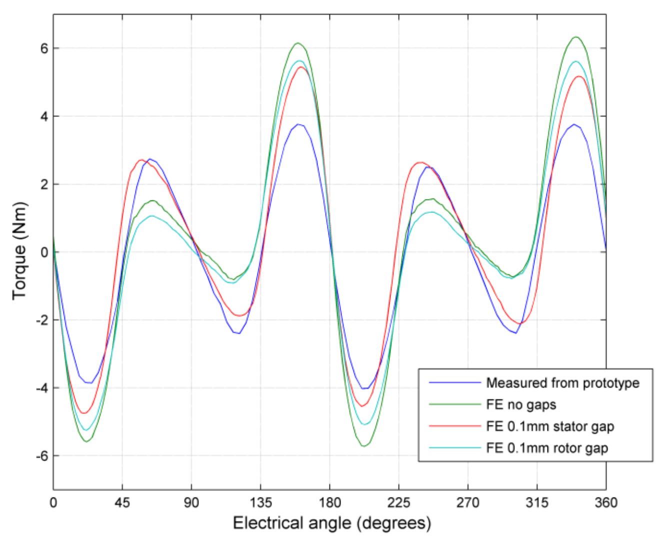

Fig. 13. Predicted cogging torque for the hybrid material machine for alternative FEA models

Comparison of initial simulation and experimental results implied FEA largely over-predicted the torque. The construction method of the prototype means that gaps between the SMC and laminate components are likely and may be significant in comparison to the active air-gap, reducing performance. The rotor assembly involved 100 small pieces being assembled onto a hub with a diameter several orders of magnitude larger than the individual pieces which will present an accumulated tolerance problem. In the stator, the sintering process of the SMC core-back arcs resulted in some deformation specifically affecting the concentric tolerance of the outer and inner radius. Although the outer diameter of the lamination rings were machined to be a good sliding fit with the SMC core-back, the lack of concentricity could not be accounted for, resulting in air-gaps at intermittent points between the two.

A study of the cogging torque was performed to quantify the effect of the size of the air-gaps between the core back and teeth sections in the stator and between the SMC pole pieces and magnets in the rotor. Fig 13. shows predicted and experimental results of introduction of a 0.1mm air-gap (in the radial direction) between the stator lamination and the SMC core-back. Peak unaligned reluctance reluctance torque either side of 90 and 270 deg clearly decreases. The introduction of a 0.1mm air-gap (circumferential direction) between all the magnets and SMC wedges in the rotor is also shown in Fig. 15. Only a small reduction in all peak cogging torques is evident compared.

Individually, neither of the air-gaps account for the cogging profile of the actual machine, although it is known from the construction that both exist. It was found that a 0.2mm air-gap between the stator laminations and the SMC core-back, coupled with a 0.1mm air-gap between all magnets and SMC wedges in the rotor gave a good correlation between simulated and measured results, shown in Fig 14, and so these values are used in the simulations.

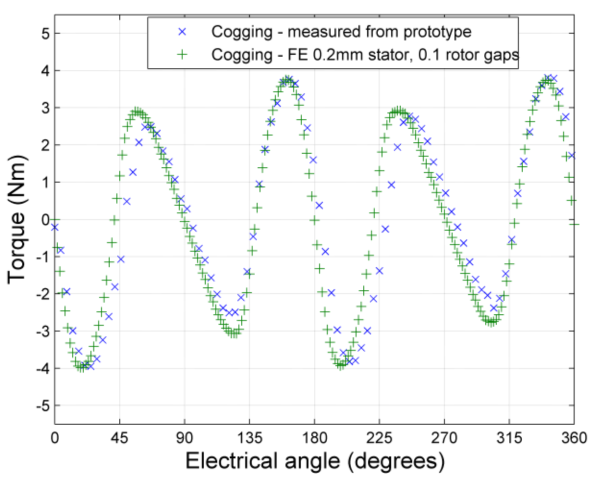

Fig. 14. Measured cogging compared to simulated with a 0.2mm stator core/teeth gap and 0.1mm rotor pole/magnet gap

In Fig. 15, the experimental verses simulated results are shown for the hybrid prototype with a fixed DC current injected into the coils. There is good agreement between the measured data and the calculated data across all angles and currents.

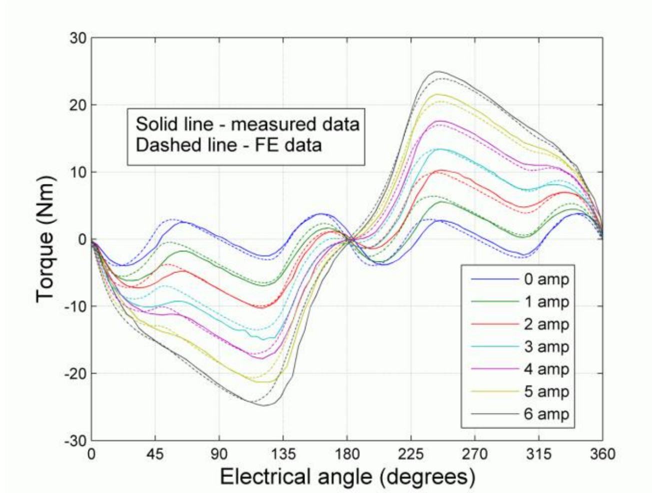

Fig. 15. Simulated and Measured Data from Hybrid Machine

Models for the other 2 machines have been similarly validated [6,15]. Experience has shown that the interface between SMC components is better than between SMC and laminations.

VI. Conclusions

This paper has discussed the materials currently utilised in the construction of MPMs, their limitations and complexities in the fabrication processes involved with each one. Simulation results have been presented, highlighting the differences in performance between each topology. Experimental results have been provided for validation of the simulation models. Measured data has been used to reveal manufacturing imperfections. As such, the calculated data includes 0.1 mm air-gaps between the rotor SMC pieces and 0.2 mm between the stator teeth and core-back in the hybrid material machine. With careful consideration of mechanical tolerances, these gaps could perhaps be removed in future models, which would alter our initial conclusions.

As they are built here, the bent lamination machine is shown to be able to deliver the highest torque per active mass, primarily due to the lack of stator coreback. The highest absolute torque is delivered by the hybrid smc/laminate machine yet it is the pure SMC version that offers the easiest machine assembly.

References

[1] H. Weh, "Acheivable Force Densities for Permanent Magnet Machines in New Configurations," in International Conference on Electrical Machines, 1986.

[2] H. Weh, H. Hoffmann, and J. Landrath, "New permanent magnet excited synchronous machine with high efficiency at low speed," in Internation Conferenece on Electrical Machines, 1988.

[3] S. Jordan and N. J. Baker, "Air-Cooled, High Torque Machines for Aerospace Applications," in 8h IET Conference on Power Electronics, Machines and Drives, Glasgow, Scotland, UK, 2016.

[4] S. Jordan and N. J. Baker, "Design and build of a mass critical, air-cooled transverse flux machine for aerospace," in 2016 XXII International Conference on Electrical Machines (ICEM), 2016, pp. 1453-1458.

[5] Z. Wan, A. Ahmed, I. Husain, and E. Muljadi, "A Novel Transverse Flux Machine for Vehicle Traction Aplications," in IEEE Power & Energy Society General Meeting, 2015, pp. 1-5.

[6] J. G. Washington, G. J. Atkinson, N. J. Baker, A. G. Jack, B. C. Mecrow, B. B. Jensen, et al., "An Improved Torque Density Modulated Pole Machine for Low Speed High Torque Applications," in 6th IET International Conference on Power Electronics, Machines and Drives, 2012, pp. 1-6.

[7] M. Gartner, P. Seibold, and N. Parspour, "Laminated Circumferential Transverse Flux Machines - Lamination Concept and Applicability to Electrical Vehicles," in IEEE International Electric Machines and Drives Conference, 2011, pp. 831-837.

[8] G. Lei, C. Liu, Y. Guo, and J. Zhu, "Multidisciplinary Design Analysis and Optimization of a PM Transverse Flux Machine With Soft Magnetic Composite Core," IEEE Transactions on Magnetics, vol. 51, pp. 1-4, 2015.

[9] C. Liu, J. Zhu, Y. Wang, G. Lei, and Y. Guo, "Cogging Torque Minimization of SMC PM Transverse Flux Machines Using Shifted and Unequal-Width Stator Teeth," IEEE Transactions on Applied Superconductivity, vol. 26, pp. 1-4, 2016.

[10] K. Sakai and J. Tanaka, "Transverse-Flux Motor for Enhanced Torque and Reduction of Torque Ripple," in 17th European Conference on Power Electronics and Applications, 2015, pp. 1-10.

[11] B. Zhang, A. S. Wang, and M. Doppelbauer, "Optimization of a Transverse Flux Machine with Claw-Pole and Flux-Concentrating Structure," in IEEE International Electric Machines & Drives Conference, 2015, pp. 1735-1741.

[12] M. F. J. Kremers, J. J. H. Paulides, and E. A. Lomonova, "Analytical 3-D design of a Transverse Flux Machine with high power factor," in 2015 International Conference on Sustainable Mobility Applications, Renewables and Technology (SMART), 2015, pp. 1-5.

[13] J. G. Washington, G. J. Atkinson, and N. J. Baker, "Reduction of Cogging Torque and EMF Harmonics in Modulated Pole Machines," IEEE Transactions on Energy Conversion, vol. 31, pp. 759-768, 2016.

[14] J. A. Walker, D. G. Dorrell, and C. Cossar, "Flux-linkage calculation in permanent-magnet motors using the frozen permeabilities method," IEEE Transactions on Magnetics, vol. 41, pp. 3946-3948, 2005.

[15] E. Pinguey, On The Design And Construction Of Modulated Pole Machines, PhD thesis, Newcastle University, 2010